



EMD Inspired by Wavelet Thresholding for Correction of Blink Artifacts from Single-Channel Cerebral Signals

Vijayasankar Anumala and Venkata Rao Dhulipalla

1 Introduction

As per the records of the WHO and the statistics of neurological disorders, 50 million people are affected by epilepsy globally and 24 million by Alzheimer's and other disorders. As a result of neurological disorders, around 6.8 million people lose their lives every year [1, 2]. Physicians suggest continuous brain monitoring to diagnose the diseases like Alzheimer's, epilepsy, and other neurological disorders.

There are several methods to acquire the cerebral activity: magnetoencephalography (MEG), functional magnetic resonance imaging (fMRI), near-infrared spectroscopy (NIRS), computed tomography (CT), electroencephalogram (EEG), etc. Though these methods can provide good spatial resolution, EEG is the powerful and frequently used tool in modern medical field and academia due to affordable price along with acceptable temporal resolution [3].

Of late, EEG-based home care systems such as Neuro Monitor and OPTIMI are being used rapidly to monitor the condition of individuals, particularly in care related to elderly, where minimal instrumentation and less computational resources are required [4, 5]. Single-channel EEG contains few electrodes and ambulatory system embedded with signal processing to process the EEG signals, which makes it more popular. EEG signal can be produced with the excitation of neurons in brain. The magnitude of the EEG signal approximately varies between $10\ \mu\text{V}$ – $100\ \mu\text{V}$ and 0–64 Hz, respectively. The sub-bands of typical EEG brain rhythms are delta, theta, alpha, and beta, respectively, from low to high frequencies which are shown in Fig. 1.

V. Anumala (✉) · V. R. Dhulipalla
Velagapudi Ramakrishna Siddhartha Engineering College,
Vijayawada, Andhra Pradesh, India
e-mail: vijayasankar.anumala@vrsiddhartha.ac.in

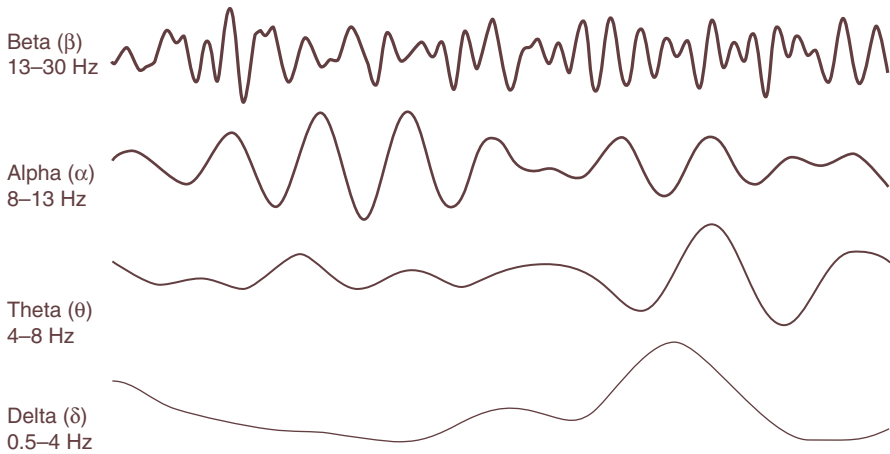


Fig. 1 Typical EEG brain rhythms

The extra-biological artifacts like line interference and electrode noise can be removed by filtering, due to spectral separation between extra-biological artifacts and electroencephalography signal. However, due to the fact that the heartbeat, movement of eyes, and muscles coexist in the frequency range as EEG signal, considerable attention must be paid to eliminate the biological artifacts. There exists a significant damage to the data of an EEG, if the procedure of artifact elimination is not methodical [6].

Several efforts have been made, and various methods have been developed till date for the removal of artifacts. However, each of them lags behind with some practical issues such as requirement of high computational resources and computational time, and there is no complete solution yet, which leads to the development of simple artifact removal techniques.

Several techniques were projected to correct BAs from recordings of EEG, among which wavelet transform (DWT and SWT) with thresholding methods is being widely used [7, 8]. Identification of mother wavelet also plays a major role in the system's overall performance.

Huang et al. developed EMD to evaluate nonstationary and nonlinear signals such as EEG [9, 10]. EMD decomposes the signal into several IMFs. The main advantage of EMD over WT is its ability to estimate suitable changes in the frequency of the signal. IMF interval thresholding is employed for correcting the artifacts resulting in a substantially cleaner EEG signal unlike using conventional EMD methods, which may result in loss of neural information at blink regions [11].

Frontal channels like F8, F7, FP2, and FP1 are likely to be dominant with respect to ocular artifacts. Thus, it is realistic to read the signals as corrupted or contaminated EEG signals from these electrodes. Figure 2 illustrates the blink artifacts of typical EEG signals. “eegmidb” (EEG motor movement/imagery) dataset was used to carry the computations [12]. Comparison is made between the proposed method and the conventional EMD with concentration on considering standard metrics for performance like ARR, RMSE, Δ SNR, and CC.

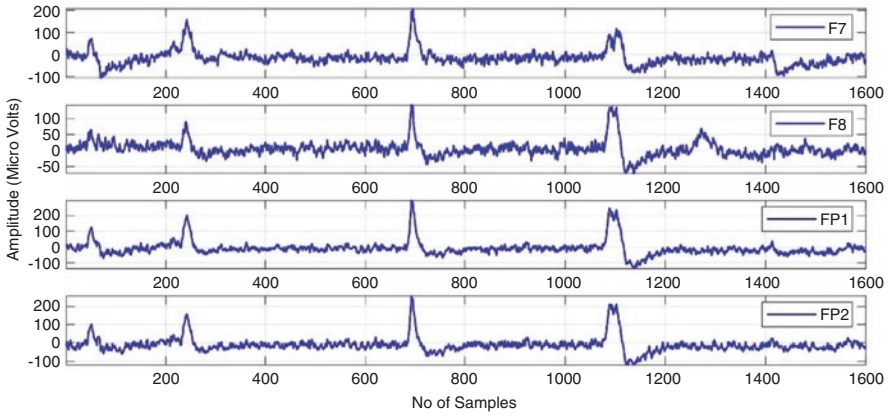


Fig. 2 Frontal electrode EEG signals with blink artifacts

The outline of this chapter is as narrated: A concise study of EMD algorithm is done in Sect. 2; Sect. 3 describes the identification of noisy IMFs and blink artifacts; the concepts of threshold function and IMF thresholding are discussed in Sect. 4; experimental verification and results of the proposed method are projected in Sect. 5; the conclusions are furnished in Sect. 6.

2 Empirical Mode Decomposition

EMD is an efficient approach for breaking down any complicated signal into finite intrinsic mode functions [13, 14]. The extremas and IMF zero crossings should be same or alter by one. The average of envelope stated by extrema must be zero at any point for each IMF. For a nonstationary signal $x(t)$, the detailed steps of EMD are the following:

- The maxima and minima points of the raw EEG signal are to be determined.
- Using cubic spline interpolation, the signals lower envelope (e_{lower}) and upper envelope (e_{upper}) are to be created.
- To generate the first IMF, the mean envelope should be deducted from the signal $x(t)$. $h_1(t) = x(t) - a(t)$, where $a(t)$ represents the average of the envelope,

$$\text{i.e., } a(t) = \frac{(e_{\text{lower}} + e_{\text{upper}})}{2}$$

- To get a new residual signal $r_1(t)$, IMF1 is to be subtracted from $x(t)$, i.e., $r_1(t) = x(t) - h_1(t)$, and then $r_1(t)$ should be decomposed as done above to obtain the second IMF.
- All the steps are to be made recurrent till no IMFs are derived. Reconstruction of original signal can be from IMFs like $x(t) = \sum_{i=1}^K h_k(t) + r(t)$. Figure 3

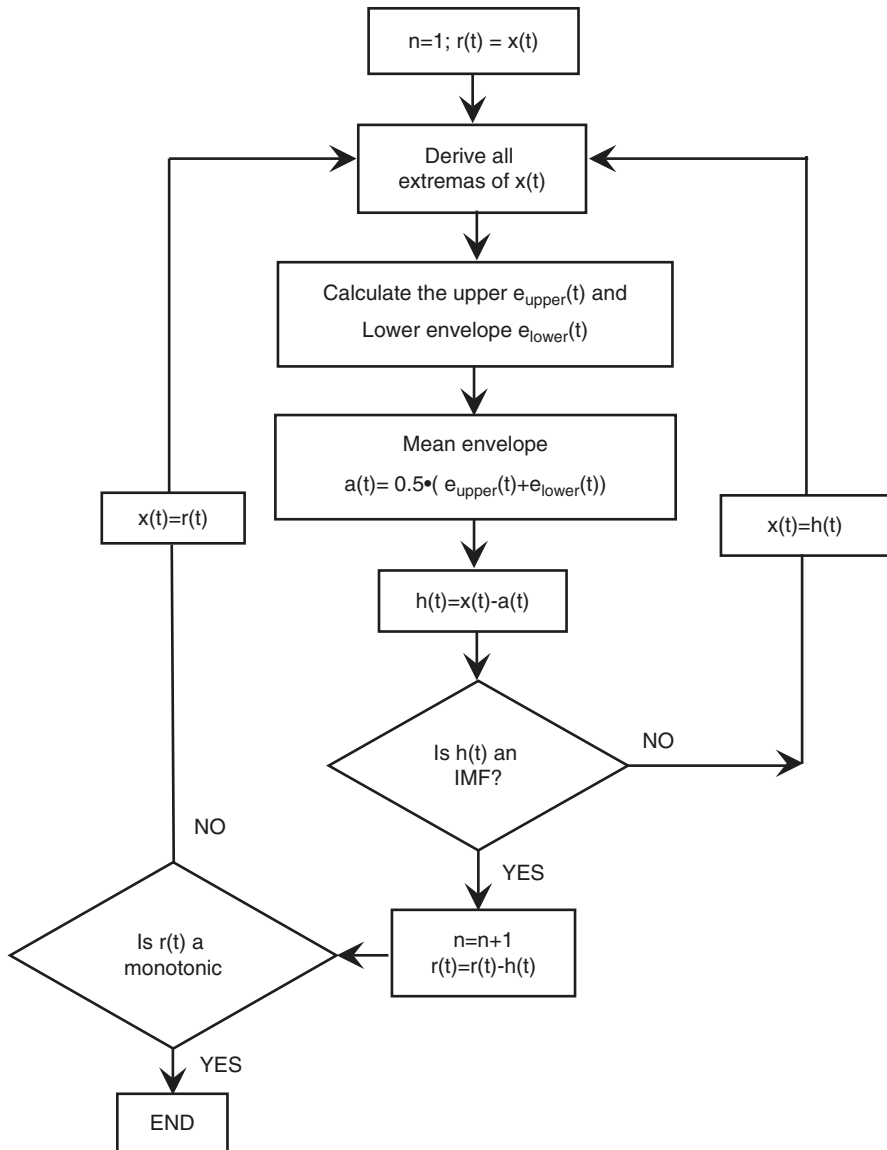


Fig. 3 Flowchart depicting the process of EMD

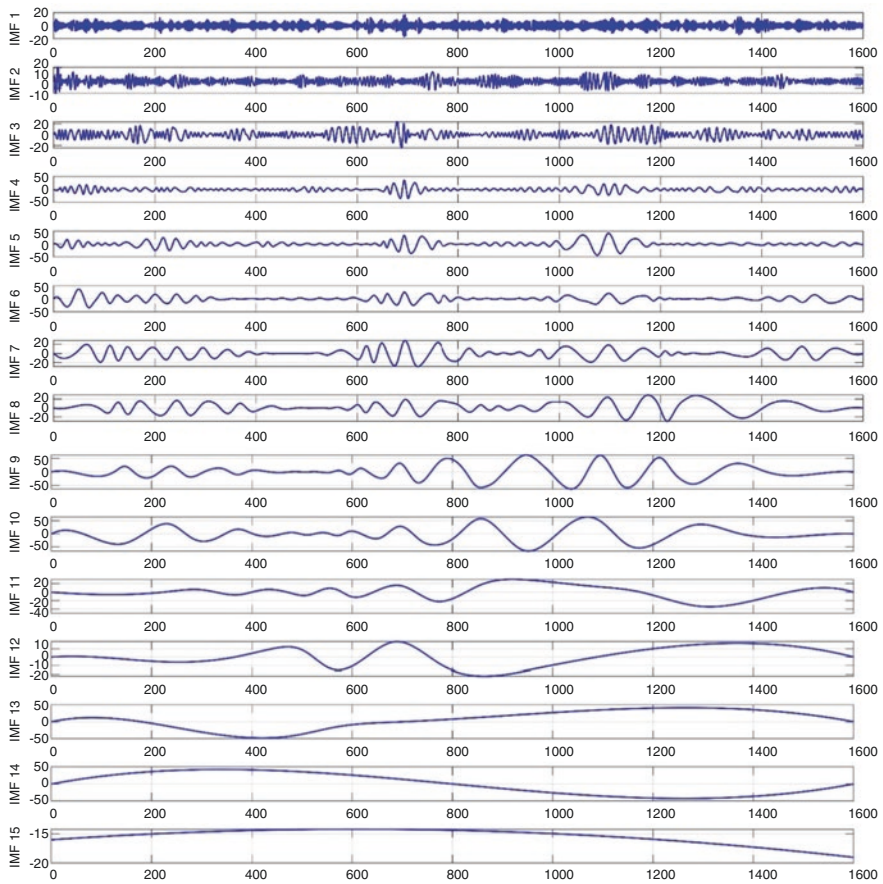


Fig. 4 IMFs 1–15 due to decomposition of FP2 EEG

illustrates the flowchart of the EMD process [15]. The resulting IMFs by applying EMD for the FP2 EEG signal are as shown in Fig. 4.

3 Identifications of Noisy IMFs and Blink Artifacts

3.1 Identification of Noisy IMFs

By performing thresholding to all IMFs, there may exist a loss of neural activity in the reconstructed signal [16]. Hence, it is necessary to identify the IMFs that belong to signal component or artifactual component and thresholding is performed to noisy IMFs that results in clearer EEG signal. The coefficients of correlation amid the IMFs and the raw EEG signal can be used to categorize the IMFs as either noise-dominant or signal-dominant modes. The magnitude and frequency of the EEG

Table 1 Correlation coefficient between raw EEG and IMFs

IMFs	1	2	3	4	5
CC	0.121	0.133	0.186	0.173	0.265
IMFs	6	7	8	9	10
CC	0.288	0.364	0.284	0.375	0.393
IMFs	11	12	13	14	15
CC	0.163	-0.045	-0.054	0.087	0.089

signal typically range from 10 μV to 100 μV and from 0 to 64 Hz, respectively, whereas ocular activity varies in the order of millivolts spread from 0 to 16 Hz sub-band. Hence, blink artifacts absolutely capture the neural signal with its occurrence, and mostly the EEG signal is noise dominant. So, the IMFs having the highest correlation coefficient with respect to raw EEG signal are considered to be dominant in noise, while the others are considered as signal dominant. However, if the signal contains a momentous noise, this method may cause some noise-dominant IMFs to be misjudged. Table 1 labels CC between the raw EEG and individual IMFs for FP2 EEG. Those IMFs with CC greater than 0.25, i.e., IMF5, IMF6, IMF7, IMF8, IMF9, and IMF10, are considered to be noise dominant.

Spectral analysis of modes is used to classify the IMFs in this study. Figure 5 illustrates the spectral comparison of raw EEG signal and its IMFs. The IMFs with substantial power at lower frequencies are considered as noisy IMFs. From this figure, IMFs 11–15 might not be considered as signal-dominant IMFs due to their spectral distribution at lower frequencies. To resolve the issue, EEG signal is pre-processed by stationary wavelet transform, and the CC between preprocessed signal and its IMFs is derived.

Raw EEG signal of sampling frequency 160 Hz is decomposed to four levels by stationary wavelet transform. Daubechies (db8) wavelet is chosen; hence, its shape resembles that of ocular activity. The approximation coefficients at fourth decomposition level that are at OA range are set to zero, and reconstruction is performed. The preprocessed EEG signal and its power spectrum are shown, respectively, in Figs. 6 and 7. As shown in Fig. 6, the spectral distribution of signal plus noise is minimum at 0–16 Hz. EMD is employed to the preprocessed signal for extracting IMFs. Correlation coefficient is carried out over the preprocessed signal and the extracted IMFs, from which noise-free IMFs are estimated and summarized in Table 2. On observing Table 1, it can be concluded that IMFs 1–4 are to be considered as signal dominant due to their mutual correlation with preprocessed signal. IMFs 11–15 are not correlated to the preprocessed signal and hence considered as noise dominant.

3.2 Identification of Blink Artifacts

Krishnaveni et al. developed a wavelet-based approach to identify slowly varying artifacts and performed denoising for the zones identified, which preserves the cerebral information at artifact-free zones. Haar wavelet is used to recognize rising and

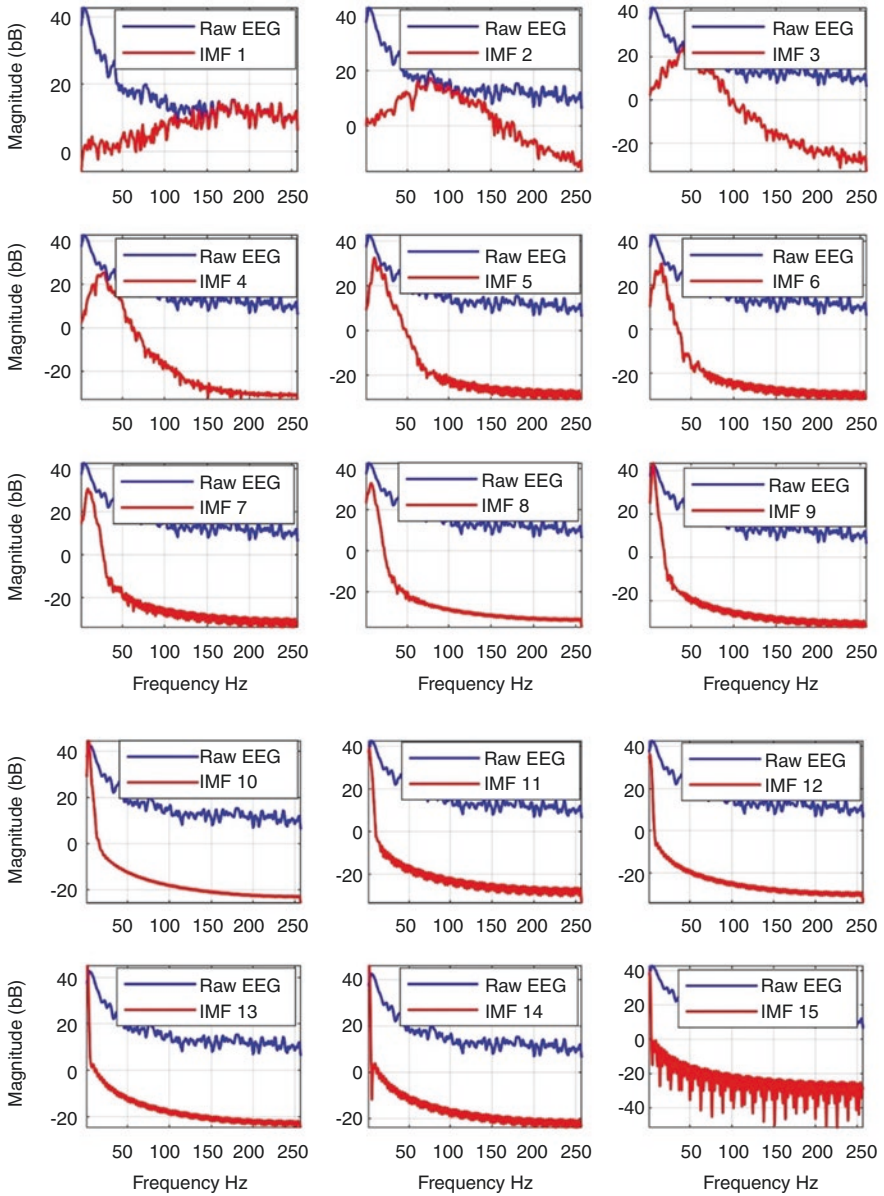


Fig. 5 Power spectral density plots of IMFs 1–15

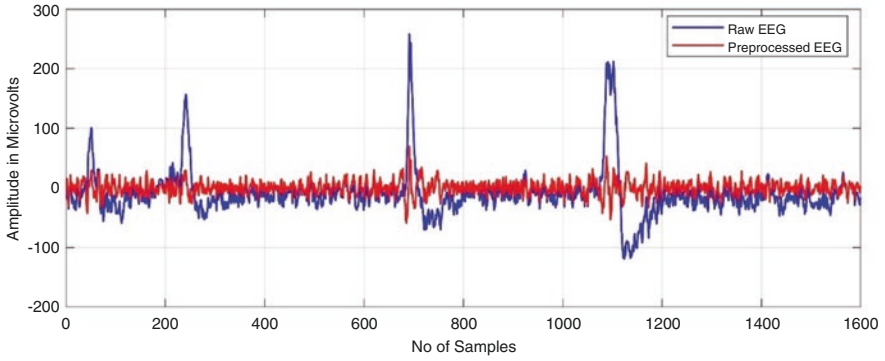


Fig. 6 Raw and preprocessed FP2 EEG signal by SWT

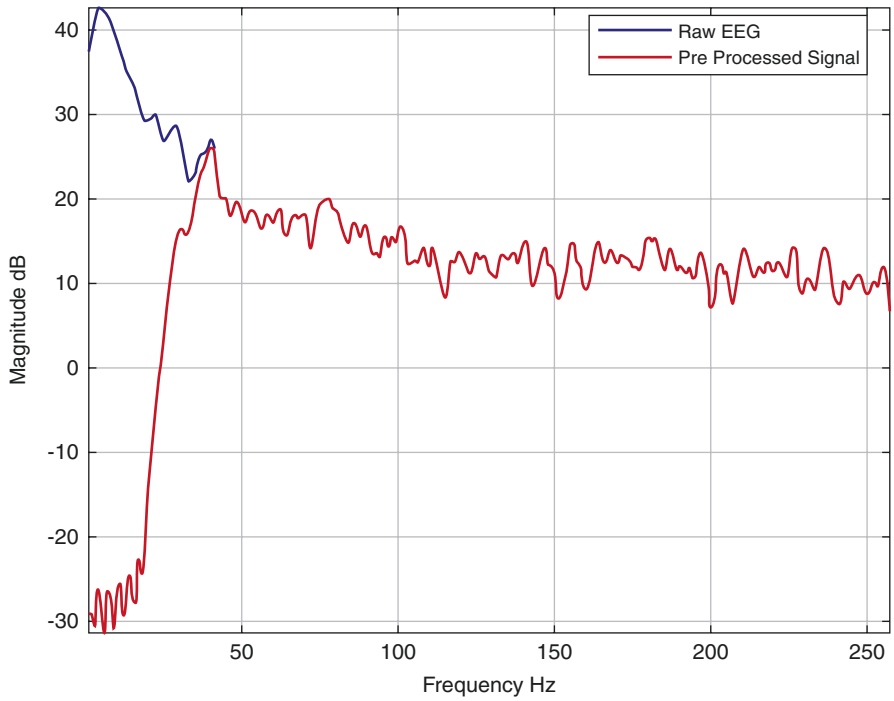
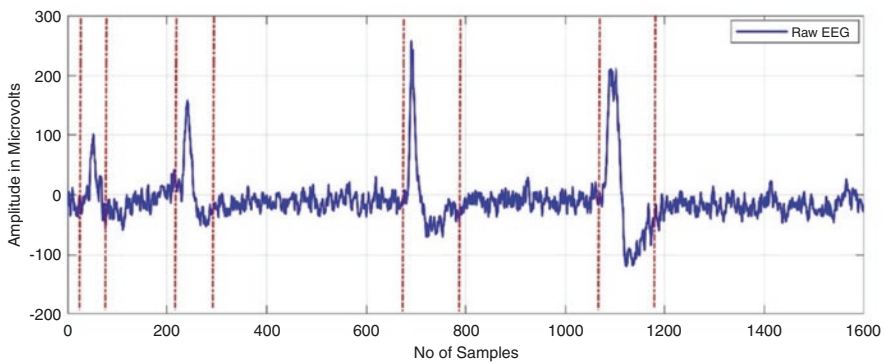


Fig. 7 Spectra of raw and preprocessed EEG signals

Table 2 Correlation coefficient between preprocessed EEG signals and its IMFs

IMFs	1	2	3	4	5
CC	0.533	0.529	0.549	0.337	0.063
IMFs	6	7	8	9	10
CC	0.004	2.05×10^{-4}	-5×10^{-5}	1.48×10^{-4}	9.9×10^{-6}
IMFs	11	12	13	14	15
CC	6.2×10^{-6}	1.48×10^{-6}	2.4×10^{-6}	4×10^{-6}	5.7×10^{-4}

**Fig. 8** Raw EEG with identified artifacts

falling edges of the blinks, i.e., artifact rising edge (ARE) and artifact falling edge (AFE); based on the location of ARE and AFE, blink zones are identified [17]. Figure 8 illustrates an EEG with identified artifacts.

4 Threshold Function and IMF Thresholding

Threshold function and thresholding methods play a critical role in artifact correction. Many threshold functions are available in literature such as universal threshold, statistical threshold, minimax threshold, and SURE threshold. But universal threshold is more popular and widely being used for artifact correction of biological signals.

4.1 Universal Threshold (UT)

UT is a function approved globally in which the threshold values for each IMF are estimated by Eq. (1):

$$\lambda_i = \sqrt{2E_i \ln N} \quad (1)$$

where E is energy and N is number of samples [18].

The energy of each IMF resulting from white Gaussian noise follows an exponential relationship defined by

$$E_i = \frac{E_1^2}{\beta} \rho^{-i} \quad i = 2, 3, \dots \tag{2}$$

Here, E_1 is the first IMF energy expressed by Eq. (3), and ρ and β are the parameters to be analyzed with a huge quantity of noise realizations and IMFs as 2.01 and 0.719, respectively [19]:

$$E_1 = \left[\frac{\text{Median} \left| h_1(n) - \overline{h_1(n)} \right|}{0.6745} \right]^2 \tag{3}$$

$h_1(n)$ replicates the first IMF coefficients. For additive white Gaussian noise, the denominator value of 0.6745 is found to be a more suitable estimator.

4.2 IMF Thresholding

The development of EMD decomposed the signal to numerous IMFs. The IMFs with higher order contain noise at low frequencies and vice versa. Typically, ocular artifacts are disseminated at 0–16 Hz. Hence, in conventional EMD, denoising of the denoised signal is attained by excluding the higher order low-frequency IMFs while combining the lower order high-frequency IMFs. However, selection of noisy IMF plays a critical role in artifact removal process; moreover, excluding the IMF completely yields loss of neural activity in artifact-free zones.

In EMD-DT (EMD direct thresholding), the signal is reconstructed after performing thresholding to the noisy IMFs. Direct wavelet thresholding performed on IMFs results in the construction of EMD-DT. The signal reconstructed with modified IMFs can be denoted as

$$x(t) = \sum_{i=M_1}^{M_2} \tilde{h}_i(t) + \sum_{i=M_2+1}^L h_i(t) + r(t) \tag{4}$$

where

$$\tilde{h}_i(t) = \begin{cases} h_i(t) & |h_i(t)| > \lambda_i \\ 0 & |h_i(t)| \leq \lambda_i \end{cases} \tag{5}$$

for hard thresholding

$$\tilde{h}_i(t) = \begin{cases} \text{sgn}(h_i(t))(|h_i(t)| - T_i) & |h_i(t)| > \lambda_i \\ 0 & |h_i(t)| \leq \lambda_i \end{cases} \tag{6}$$

for soft thresholding.

M_2 and M_1 , respectively, indicate the high-order, low-order IMFs. λ_i is the value of threshold at i th IMF. However, for the decomposition modes, directly applying the threshold can yield disastrous results to disturb the continuity of the signal reconstructed. Kopsinis and Mclanglin introduced and verified an innovative EMD-based denoising technique on different signals, where EMD-IT was studied [20–22]. Taking into note the two zero crossings (adjacent) $Z_j^{(i)} = [Z_j^{(i)} Z_j^{(i+1)}]$ in the i th IMF, hard and soft thresholding for the IMF coefficients can be described mathematically by Eqs. (7) and (8), respectively:

$$\tilde{h}_i(z_j^i) = \begin{cases} h_i(z_j^i) & |h_i(r_j^i)| > \lambda_i \\ 0 & |h_i(r_j^i)| \leq \lambda_i \end{cases} \tag{7}$$

$$\tilde{h}_i(z_j^i) = \begin{cases} h_i(z_j^i) \frac{(|h_i(r_j^i)| - T_i)}{|h_i(r_j^i)|} & |h_i(r_j^i)| > \lambda_i \\ 0 & |h_i(r_j^i)| \leq \lambda_i \end{cases} \tag{8}$$

where h_i is the IMF coefficient before decomposition, \tilde{h}_i is the estimated IMF coefficient after thresholding, $h_i(z_j^i)$ indicates the samples from z_j^i to z_j^{i+1} , and $h_i(r_j^i)$ represents the maxima of the zero crossing interval. Hard thresholding is unstable and is sensitive to even minute modifications of the signal: i.e., the coefficients remain unchanged above the threshold and below are decreased to zero. The local properties of the signal are not modified by this method, but due to discontinuity, they lead to certain fluctuation in the reconstructed signal. Soft thresholding is more stable than hard thresholding, and the coefficients can be minimized towards zero. Hence, soft thresholding is selected throughout, for this study.

The modified IMF coefficients by direct and interval thresholding for IMF 5 are as shown in Fig. 9. T_5 is the obtained threshold value of fifth IMF using universal threshold. The modified IMF coefficients are continued at zero crossing by direct

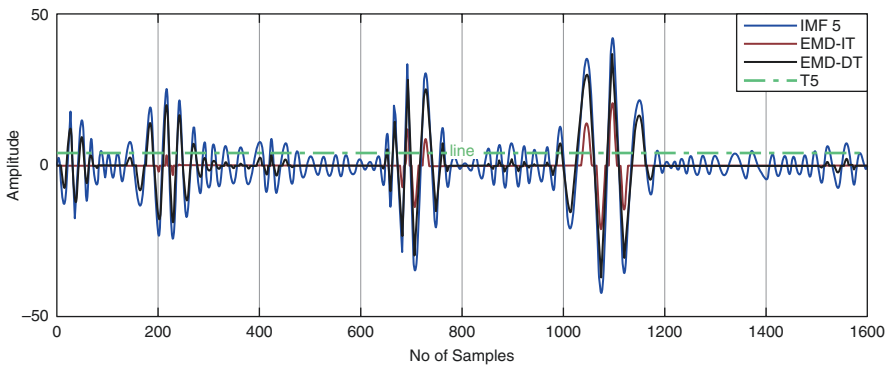


Fig. 9 Modified IMF coefficients by EMD-DT and EMD-IT techniques

thresholding, whereas those in the neighborhood of zero crossings are reduced to zero by interval thresholding, resulting in errors in the reconstructed signal. Hence, EMD direct thresholding is not a suitable choice for correcting artifacts of EEG signals.

4.3 Methodology

EMD is to be performed on the raw EEG signal for extracting the IMFs. The IMFs with higher order contain noise at low frequencies and vice versa; that is, the BAs are found to be distributed in the higher order IMFs.

The noisy IMFs are to be identified as explained in Sect. 3.1.

The threshold for each IMF should be calculated, and interval thresholding for the identified noisy IMFs is performed as described in Sect. 4.2.

Modified IMFs and the remaining signal IMFs are added for reconstructing the signal according to Eq. (4).

The metrics ARR, Δ SNR, RMSE, and CC amid clean and raw EEG signals are to be calculated. Figure 10 depicts the process of artifact correction.

5 Experimental Verification and Results

The quantitative metrics to evaluate the denoising techniques are defined by the following equations [23]:

$$\Delta \text{SNR} = 10 \log_{10} \left(\frac{\sigma_x^2}{\sigma_y^2} \right) \quad (9)$$

$$\text{ARR} = \frac{\sum_{i=1}^N (x_i(n) - y_i(n))^2}{\sum_{i=1}^N y_i^2(n)} \quad (10)$$

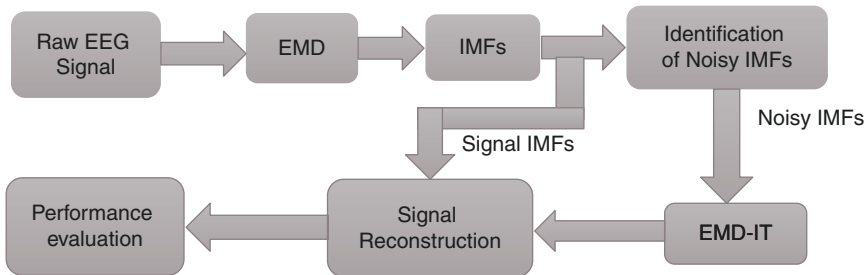


Fig. 10 Denoising approach based on EMD-IMF thresholding

$$CC = \frac{\sum_{n=1}^N (x[n] - \overline{x[n]})(y[n] - \overline{y[n]})}{\sqrt{\sum_{n=1}^N (x[n] - \overline{x[n]})^2 \sum_{n=1}^N (y[n] - \overline{y[n]})^2}} \quad (11)$$

$$RMSE = \sqrt{\frac{1}{N} \sum_{n=1}^N (x[n] - y[n])^2} \quad (12)$$

where $y(n)$ represents the clean EEG signal, $x(n)$ is the contaminated EEG, and σ_y^2 and σ_x^2 are the variance of the clean and raw EEG signals, respectively.

5.1 Results and Discussions

In the conventional EMD-based denoising method, the denoised signal is the sum of selected IMFs by excluding the IMFs which have artifactual components. However, in EMD direct thresholding (EMD-DT), the signal is reconstructed after performing thresholding to the noisy IMFs. Figure 11 exemplifies the raw and reconstructed FP2 EEG signal with EMD-DT and conventional EMD denoising method of artifact correction. Artifacts in blink region are not suppressed by EMD-DT method, which can be done by conventional EMD method. However, the cerebral activity at artifact-free zones might be affected. Table 3 represents the quantitative metrics between the contaminated and clean EEG signals, using conventional EMD and EMD-DT techniques for the frontal EEG signals at non-blink regions, which are separately discussed in Sect. 3.2, with an average CC and RMSE of 0.4175, 0.84 and 21.55, 0.443 by conventional EMD and EMD-DT methods, respectively, over non-blink regions. Artifacts are largely attenuated by the conventional EMD method, but the neural information is greatly affected based on CC and RMSE.

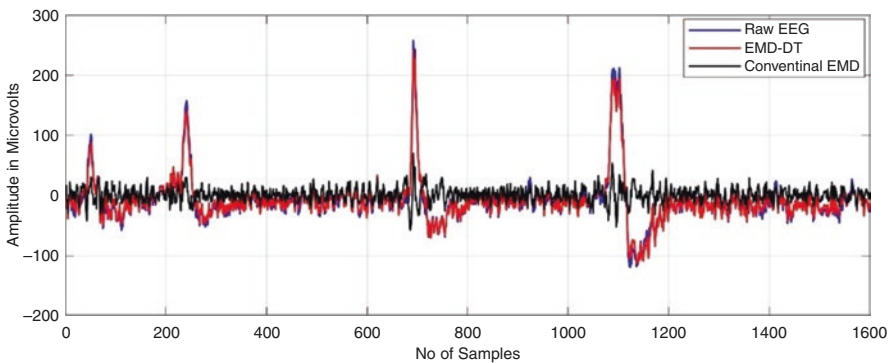


Fig. 11 Clean EEG signal by the conventional EMD method

Table 3 Quantitative metrics of artifact removal by Conv-EMD and EMD-DT

Channel	Conv-EMD		EMD-DT	
	CC	RMSE	CC	RMSE
F7	0.40	21.64	0.82	2.46
F8	0.36	16.87	0.84	2.43
FP1	0.44	26.86	0.86	3.24
FP2	0.47	20.86	0.85	3.16

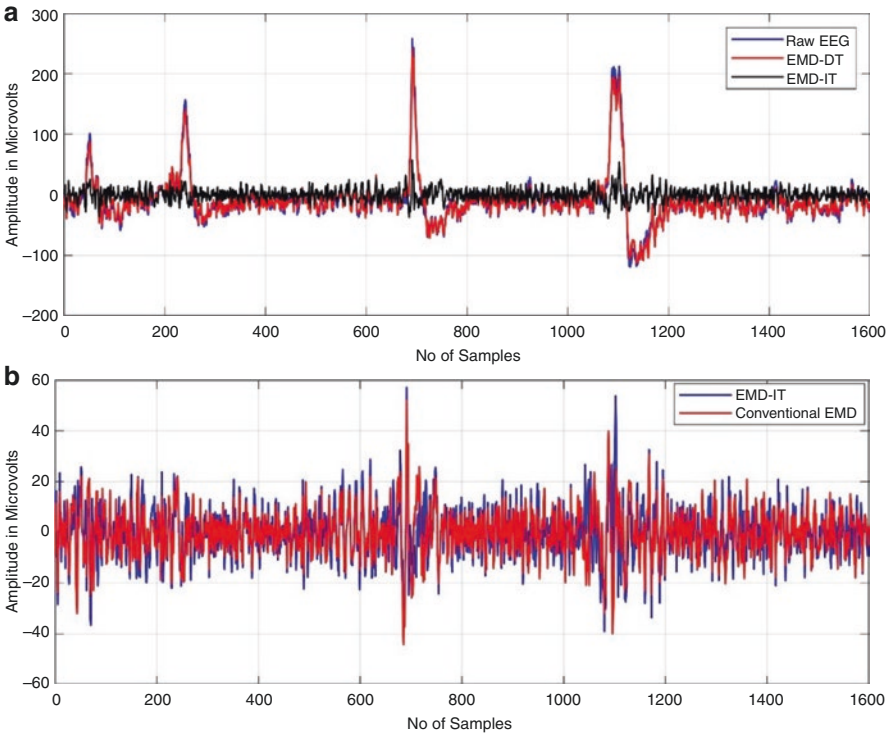


Fig. 12 (a) Clean EEG signal by EMD-IT and EMD-DT techniques. (b) Clean FP2 EEG signal by Conv-EMD and EMD-IT techniques

However, in the partial sum of IMFs, there might be the possibility of excluding high-frequency content in the signal or including the unwanted low-frequency oscillations of the signal. With this view to avoid any loss of data in the signal reconstructed, IMF interval thresholding is opted for artifact correction.

Figure 12 illustrates the time domain description of FP2 EEG signal before and after artifact removal by conventional EMD, EMD-DT, and EMD-IT methods.

Table 4 Δ SNR, ARR, CC, and RMSE by EMD-DT and EMD-IT methods

Channel	EMD-DT				EMD-IT			
	Δ SNR	ARR	CC	RMSE	Δ SNR	ARR	CC	RMSE
F7	1.12	1.24	0.82	2.46	19.24	8.26	0.64	28.22
F8	0.98	1.18	0.84	2.43	18.06	7.98	0.68	28.38
FP1	1.15	1.54	0.86	3.24	23.70	14.8	0.66	32.46
FP2	1.22	1.46	0.85	3.16	23.25	13.57	0.65	34.42

From this figure, it can be clearly understood that EMD-DT method is unable to reject the artifacts, whereas conventional EMD and EMD-IT methods minimize the artifacts to a greater extent.

Table 4 provides the average quantitative metrics between contaminated and reconstructed EEG signals using EMD-DT and EMD-IT techniques. The higher the values of Δ SNR and ARR, the better will be the rejection of artifacts, the higher the CC, and the lower the RMSE, which indicate that the neural information is protected. Δ SNR and ARR are estimated for the whole data, whereas CC and RMSE are estimated at non-blink regions. EMD-DT and EMD-IT methods have accounted for average Δ SNR, ARR, CC, and RMSE of 1.11, 1.35, 0.84, and 2.82 and 21.05, 11.15, 0.65, and 30.8, respectively, for the frontal EEG signals. According to Δ SNR and ARR, EMD-IT method has given better results than EMD-DT. Similarly, the performance of EMD-DT is found superior to EM-IT considering CC and RMSE. Universal threshold opted for DT was unable to shrink the IMF coefficients at each level, thereby being incapable to reject the artifacts. However, the same threshold function shrinks the coefficients better by the process of interval thresholding between zero crossings. CC and RMSE for EMD-IT are poor compared to EMD-DT but superior to conventional EMD method of artifact correction.

Blink artifacts were found dominant in EEG recording and occupy the low-frequency band from 0 to 16 Hz. Artifact removal algorithms should selectively reduce the spectral power in the lower frequency bands without distressing the high-frequency bands. Hence, spectral analysis was carried out for the EEG signal to estimate the artifact correction in the frequency domain, which is implemented in this study using Welch method (pwelch). Figure 13 illustrates power spectral density (PSD) of the raw and reconstructed EEG signals using EMD-DT and EMD-IT techniques. Unlike the spectrum of FP2 EEG signal, the power drop is found restricted to lower frequencies, and the neural information at higher frequencies is preserved by EMD-IT method.

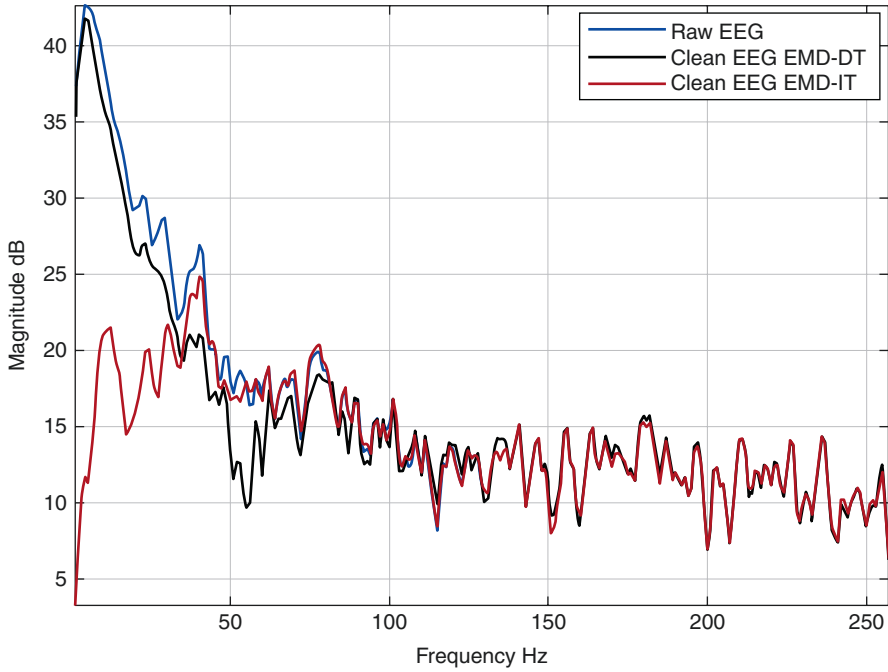


Fig. 13 Spectra of raw and clean EEG signals by EMD-DT and EMD-IT methods

6 Conclusion

In this chapter, IMF interval thresholding is proposed to correct blink artifacts of EEG signals. Noisy IMFs are detected based on CC and power spectral density estimate of the signals. Background data at artifact-free regions is conserved by performing thresholding to the noisy IMFs. Performance of the proposed method is compared with EMD-DT and conventional method of EMD denoising in terms of several standard metrics: ARR, Δ SNR, RMSE, and CC. Conventional EMD denoising method has shown extreme performance in artifact rejection, utterly affecting the neural activity. EMD-DT can preserve the neural information at artifact-free zones but is unable to correct the artifacts, whereas EMD-IT is good in correcting the artifacts while preserving the cerebral information at artifact-free regions. However, the neural information at non-blink regions is further improved by an optimized threshold function.

References

1. World Health Organization (WHO). Neurological disorders: public health challenges. Geneva: WHO; 2006.
2. Chin JH, Vora N. The global burden of neurologic diseases. *Neurology*. 2014;83(4):349–51.

3. Teplan M. Fundamentals of EEG measurement. *Measur Sci Rev.* 2002;2(2):1–11.
4. Peng H, Hu B, Shi Q, Ratcliffe M, Zhao Q, Qi Y, Gao G. Removal of ocular artifacts in EEG-an improved approach combining DWT and ANC for portable applications. *IEEE J Biomed Health Inform.* 2107;17(3):600–7.
5. Zhao Q, Hu B, Shi Y, Li Y, Moore P, Sun M. Automatic identification and removal of ocular artifacts in EEG-improved adaptive predictor filtering for portable applications. *IEEE Trans Nano Biosci.* 2014;13:109–17.
6. Savelainen A. An introduction to EEG artifacts. Aalto University School of Science: Systems Analysis Laboratory. 2010;20:1–22.
7. Sundararajan D. Discrete wavelet transform: a signal processing approach. Singapore: John Wiley & Sons; 2015.
8. Krishnaveni V, Jayaraman S. Automatic identification and removal of ocular artifacts from EEG using wavelet transform. *Measur Sci Rev.* 2006;6(4):45–57.
9. Huang NE, Shen Z, Long SR, Wu MC, Shih HH, Zheng Q, Yen N-C, Tung CC, Liu HH. The empirical mode decomposition and the Hilbert spectrum for nonlinear and non-stationary time series analysis. *Proc Roy Soc A Math Phys Eng.* 1998;454:903–95.
10. Boudraa AO, Cexus JC. EMD-based signal filtering. *IEEE Trans Instrum Meas.* 2007;56(6):2196–202.
11. Kopsinis Y, McLaughlin S. Empirical mode decomposition based denoising techniques. In *Proc. 1st IAPR Workshop Cogn. Inf. Process. (CIP)*, Santorini, Greece, Jun 2008, pp. 42–47.
12. Goldberger AL, Amaral LAN, Glass L, Hausdorff JM, Ivanov PC, Mark RG, Mietus JE, Moody GB, Peng C-K, Stanley HE. PhysioBank, PhysioToolkit, and PhysioNet: components of a new research resource for complex physiologic signals. *Circulation.* 2000;101:215–20.
13. Elouaham S, Latif R, Laaboubi A, Maoulainine FMR. Biomedical signals analysis using the empirical mode decomposition and parametric and non-parametric time -frequency techniques. *Int J on Inform Technol.* 2013;1:1–10.
14. Flandrin P, Rilling G, Goncalves P. Empirical mode decomposition as a filter bank. *IEEE Signal Process Lett.* 2004;11:112–4.
15. Khan Z, Keshava Murthy GN. Correction of ocular artifacts in EEG signal using empirical mode decomposition and cross-correlation. *Res J Biotechnol.* 2014;9(12):24–9.
16. Cheng J, Yu D. Research on the intrinsic mode function (IMF) criterion in EMD method. *Mech Syst Signal Process.* 2006;20(4):817–24.
17. Krishnaveni V, Jayaraman S, Aravind S, Hariharasudhan V, Ramadoss K. Automatic identification and removal of ocular artifacts from EEG using wavelet transform. *Measur Sci Rev.* 2006;6(4):45–57.
18. Donoho DL. Denoising by soft-thresholding. *IEEE Tran Inf Theory.* 1995;41:613–27.
19. Flandrin P, Rilling G, Gonçalvès P. EMD equivalent filter banks, from interpretation to applications. In: *Hilbert-Huang transform and its applications.* Singapore: World Scientific; 2005.
20. Kopsinis Y, McLaughlin S. Development of EMD-based Denoising methods inspired by wavelet thresholding. *IEEE Trans Signal Process.* 2009;57(4):1351–62.
21. Yang G, Liu Y, Wang Y, Zhu Z. EMD interval thresholding denoising based on similarity measure to select relevant modes. *Signal Processing;* 2014. p. 1–15.
22. Zhang M, Guo W. An integrated EMD adaptive threshold denoising method for reduction of noise in ECG. *PLoS One.* 2020:1–30.
23. Valipour S, Kulkarni GR, Shaligram AD. Study on performance metrics for consideration of efficiency of the ocular artifact removal algorithms for EEG signals. *Indian J Sci Technol.* 2015:1–6.